Two Robust Interstellar Meteor Candidates in the Post-2018 CNEOS Fireball Database

Richard Cloete[1] and Abraham Loeb[1]

[1]*Astronomy Department, Harvard University, 60 Garden Street, Cambridge, MA, 02138, USA*

ABSTRACT

We report the identification of two previously unrecognized interstellar meteor candidates in the NASA CNEOS fireball database. Exploiting the empirically calibrated low-discrepancy uncertainty model of Peña-Asensio et al. (2025), which characterizes post-2018 CNEOS velocity accuracy at $\sigma_v = 0.55$ km s^{-1}, $\sigma_{\rm RA} = 1.35°$, $\sigma_{\rm Dec} = 0.84°$, we transform CNEOS velocity vectors to heliocentric orbits and assess interstellar candidacy via 10^6-draw Monte-Carlo simulations. Two post-2018 events have heliocentric speeds robustly exceeding the escape velocity from the Solar System. CNEOS-22 (2022-07-28; 6.0°S, 86.9°W; eastern tropical Pacific) has $v_\odot = 46.98$ km s^{-1}, exceeding solar escape by $\langle \Delta \rangle = 5.18 \pm 0.60$ km s^{-1} ($z_\Delta = 8.7\sigma$), with heliocentric interstellar speed $v_{\infty,\odot} = 21.5$ km s^{-1}. CNEOS-25 (2025-02-12; 73.4°N, 49.3°E; Barents Sea) has $v_\odot = 45.63$ km s^{-1}, exceeding escape by $\langle \Delta \rangle = 3.22 \pm 0.58$ km s^{-1} ($z_\Delta = 5.5\sigma$), with $v_{\infty,\odot} = 16.9$ km s^{-1}. For both events, none of 10^6 Monte-Carlo realizations yield an orbit that is gravitational bound to the Solar System ($p_{\rm bound} < 3 \times 10^{-6}$). The adopted error model would need to underestimate the true uncertainties by factors of 5–9 for either candidate's unbound status to be marginal.

Keywords: interstellar objects — meteors — meteoroids — fireballs

1. INTRODUCTION

The discoveries of 1I/'Oumuamua (K. J. Meech et al. 2017), 2I/Borisov (P. Guzik et al. 2020), and 3I/ATLAS (D. Z. Seligman et al. 2025) demonstrated that large ($\gtrsim 0.1$ km) interstellar objects transit the inner Solar System. Although smaller bodies evade telescope detection, they can reveal themselves as fireballs when they enter Earth's atmosphere at speeds exceeding the local escape velocity from the Solar System.

The CNEOS fireball database, maintained by NASA's Jet Propulsion Laboratory, is a global, space-based catalog providing event-level velocity vectors for bolide detections from U.S. Government sensors. These velocity measurements enable computation of heliocentric orbits and testing whether an impactor was gravitationally unbound to the Sun. However, CNEOS publishes no per-event uncertainties, and the accuracy of reported velocities has varied across sensor generations.

Previous interstellar meteor reports have focused on IM1 from 2014-01-08 (A. Siraj & A. Loeb 2022a) and IM2 from 2017-03-09 (A. Siraj & A. Loeb 2022b; E. Peña-Asensio et al. 2022), based on nominal heliocentric speeds exceeding escape velocity. Independent analysis

of IM1 by the U.S. Space Command confirmed its interstellar identification[2], but others raised concerns about the velocity accuracy of pre-2018 CNEOS data (H. A. Devillepoix et al. 2019), arguing that without a calibrated uncertainty model, it is impossible to distinguish genuinely unbound trajectories from measurement artifacts.

The situation improved substantially with the empirical calibration of E. Peña-Asensio et al. (2025a), who cross-matched CNEOS events with independent ground-truth networks. Their analysis reveals two regimes: a high-discrepancy regime for pre-2018 events (speed errors $\sigma_v \sim 6$ km s^{-1}, radiant uncertainties of tens of degrees) and a *low-discrepancy* regime for post-2018 events ($\sigma_v \approx 0.55$ km s^{-1}, $\sigma_{\rm RA} \approx 1.35°$, $\sigma_{\rm Dec} \approx 0.84°$). This calibration provides, for the first time, an empirically grounded basis for formal statistical assessment of interstellar candidacy.

In this Letter, we report two previously unrecognized post-2018 CNEOS fireballs whose heliocentric speeds robustly exceed the solar escape velocity under the calibrated low-discrepancy error model. Both events remain unbound to the Solar System in 10^6 Monte-Carlo re-

Email: aloeb@cfa.harvard.edu

[2] https://lweb.cfa.harvard.edu/~loeb/DoD.pdf

alizations, with many-sigma margins above the escape speed.

2. DATA AND ANALYSIS

2.1. CNEOS Data and Ephemerides

We analyze the complete CNEOS fireball catalog, retaining events with reported latitude, longitude, altitude, and three-component velocity vectors. For each event, the Earth-fixed (ITRS) velocity is transformed to inertial geocentric (GCRS) coordinates using Astropy (A. Collaboration et al. 2022), accounting for Earth rotation, precession, nutation, and polar motion. Earth's gravitational influence is removed via a two-body hyperbolic model to obtain the geocentric excess velocity $\mathbf{v}_{\infty,\oplus}$. The heliocentric velocity is then $\mathbf{v}_{\odot} = \mathbf{v}_{\infty,\oplus} + \mathbf{v}_E$, where $\mathbf{v}_E$ is the Earth's heliocentric velocity from JPL Horizons (J. Giorgini et al. 1996) at the event time. An event is classified as an interstellar candidate when $|\mathbf{v}_{\odot}| > v_{\mathrm{esc},\odot}(r_E) = \sqrt{2GM_{\odot}/r_E} \approx 42 \mathrm{~km\,s^{-1}}$, where r_E is the Earth-Sun separation at the event time.

2.2. Uncertainty Propagation

We adopt the low-discrepancy uncertainties from E. Peña-Asensio et al. (2025a): $\sigma_v = 0.55 \mathrm{~km\,s^{-1}}$ (speed), $\sigma_{\mathrm{RA}} = 1.35°$, $\sigma_{\mathrm{Dec}} = 0.84°$ (radiant direction), and restrict our candidacy claims to the post-2018 era where these values apply.

For each candidate, we perform $N = 10^6$ Monte-Carlo realizations. In each draw, the geocentric speed magnitude is perturbed by $\mathcal{N}(0, \sigma_v)$ (normal distribution) and the velocity direction is perturbed on the tangent plane with per-axis angular uncertainty $\sigma_{\theta,\mathrm{axis}} = \sqrt{(\sigma_{\mathrm{RA}}^2 + \sigma_{\mathrm{Dec}}^2)/2} \approx 1.12°$. The full orbit computation chain is re-evaluated for each realization.

We report two statistics: (1) the fraction of realizations yielding unbound orbits, with the rule-of-three providing a 95% upper limit on p_{bound} when zero bound draws are observed; and (2) the continuous margin $\Delta = (v_{\odot} - v_{\mathrm{esc},\odot})$, whose significance $z_{\Delta} = \langle\Delta\rangle/\sigma_{\Delta}$ expresses the mean excess above escape in units of its Monte-Carlo scatter.

3. RESULTS

Restricting attention to the post-2018 low-discrepancy era, two events emerge as robust interstellar candidates. Both have positive heliocentric specific energy at their nominal velocities and remain unbound to the Solar System in all 10^6 Monte-Carlo realizations. Neither has been previously identified as an interstellar candidate. Figure 1 places both events in context of the full post-2018 catalog.
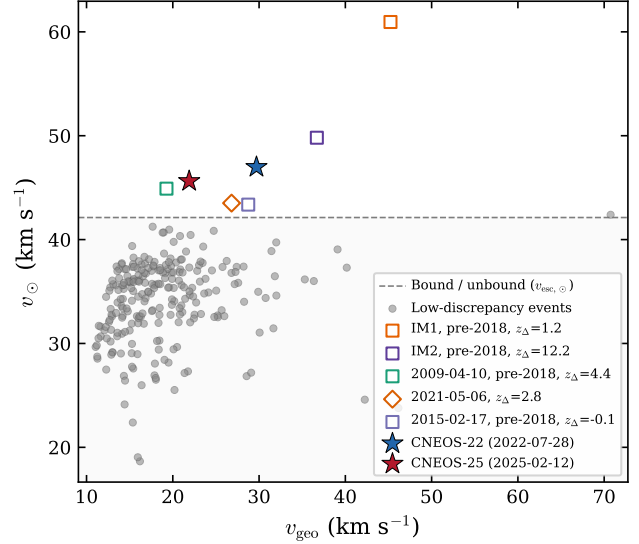

Figure 1. Heliocentric speed $v_{\odot}$ versus geocentric speed v_{geo} for CNEOS fireballs with complete velocity vectors. The horizontal dashed line marks the bound/unbound boundary at the solar escape speed $v_{\mathrm{esc},\odot} \approx 42 \mathrm{~km\,s^{-1}}$. Grey circles are low-discrepancy events with bound nominal orbits. Several events lie above the boundary at their nominal velocities (individual legend entries): pre-2018 events (open squares), including IM1 and IM2, and a post-2018 marginal event (open diamond). CNEOS-22 (2022-07-28) and CNEOS-25 (2025-02-12) (colored stars) are the only post-2018 events that remain robustly unbound across all 10^6 Monte-Carlo realizations ($z_{\Delta} > 5$; $p_{\mathrm{bound}} < 3 \times 10^{-6}$).

3.1. CNEOS-22: 2022-07-28

This fireball occurred at 01:36:07 UTC over the eastern tropical Pacific Ocean (6.0°S, 86.9°W), approximately 600 km west of Peru, at an altitude of 37.5 km. Its impact energy of 0.69 kt places it comfortably above the 0.45 kt secondary low-discrepancy threshold. The CNEOS velocity components are $(v_x, v_y, v_z) = (-17.1, +23.5, -7.2) \mathrm{~km\,s^{-1}}$.

After coordinate transformation, Earth gravity removal, and heliocentric vector addition, the heliocentric speed is $v_{\odot} = 46.98 \mathrm{~km\,s^{-1}}$, exceeding the solar escape speed of $v_{\mathrm{esc},\odot} = 41.79 \mathrm{~km\,s^{-1}}$ by 5.19 km s^{-1}. The heliocentric excess speed is $v_{\infty,\odot} = 21.5 \mathrm{~km\,s^{-1}}$ and the specific orbital energy is $\varepsilon_{\odot} = +230 \mathrm{~km^2\,s^{-2}}$.

Under the Monte-Carlo analysis, $\langle v_{\odot}\rangle = 46.98 \pm 0.60 \mathrm{~km\,s^{-1}}$ and the margin $\langle\Delta\rangle = 5.18 \pm 0.60 \mathrm{~km\,s^{-1}}$ ($z_{\Delta} = 8.7$). None of 10^6 draws yield an orbit bound to the Solar System.

The impact energy and speed imply a bolide with a mass of 6.4×10^6 g and a radius of 91 cm $\times$ $(\rho/2 \mathrm{~g\,cm^{-3}})^{-1/3}$ for a solid density ρ. The air's ram-

pressure at the fireball's peak-brightness altitude was 5.2 MPa.

3.2. CNEOS-25: 2025-02-12

This fireball occurred at 04:33:39 UTC over the Barents Sea (73.4°N, 49.3°E), between Novaya Zemlya and Franz Josef Land in the high Arctic, at 42.0 km altitude. Its impact energy is 0.13 kt; it qualifies for the low-discrepancy regime by its post-2018 date. The CNEOS velocity components are $(v_x, v_y, v_z) = (+9.5, +19.6, -1.9)$ km s^{-1}.

The heliocentric speed is $v_\odot = 45.63$ km s^{-1}, exceeding the escape speed of $v_{esc,\odot} = 42.40$ km s^{-1} by 3.23 km s^{-1}. The heliocentric excess speed is $v_{\infty,\odot} = 16.9$ km s^{-1} and $\varepsilon_\odot = +142$ km^2 s^{-2}.

Under the Monte-Carlo analysis, $\langle v_\odot \rangle = 45.62 \pm 0.58$ km s^{-1} and $\langle \Delta \rangle = 3.22 \pm 0.58$ km s^{-1} ($z_\Delta = 5.5$). None of 10^6 draws yield a bound orbit.

The impact energy and speed imply a bolide with a mass of 2.2×10^6 g and a radius of 64 cm $\times$ $(\rho/2$ g cm$^{-3})^{-1/3}$ for a solid density ρ. The air's ram-pressure at the fireball's peak-brightness altitude was 1.5 MPa.

3.3. Summary

Table 1 presents the key properties of both candidates. For each, the 95% upper limit on the bound probability is $p_{bound} < 3 \times 10^{-6}$ (rule of three for 0 in 10^6 trials). The margin significances of 8.7σ and 5.5σ quantify how deeply into the unbound regime each event lies, independent of the Monte-Carlo sample size. The Monte-Carlo velocity distributions are shown in Figure 2.

4. DISCUSSION

4.1. Robustness and Systematics

Our results are conditional on the E. Peña-Asensio et al. (2025a) low-discrepancy error model. If the true uncertainties for these events are larger than adopted, the inferred bound fractions would increase. However, the error model would need to underestimate the true uncertainties by a factor of $\sim$8.7 for CNEOS-22 and $\sim$5.5 for CNEOS-25 before the mean margin drop to 1σ— inflation factors inconsistent with the calibration data. Figure 3 quantifies this: both candidates maintain $z_\Delta > 3$ until the uncertainties are inflated by factors of $\sim$2–3, and CNEOS-22 remains above 1σ even at $\sim$9$\times$ inflation.

The CNEOS velocities are measured at peak brightness after some atmospheric deceleration. The reported speeds are therefore *lower bounds* on the true entry speeds, and a correction would only strengthen the unbound classifications. Similarly, the two-body approximations used for Earth gravity removal and the solar

binding test introduce sub-percent velocity corrections, negligible compared to the km s^{-1} measurement uncertainties.

4.2. Comparison with Known Interstellar Objects

The heliocentric interstellar speeds of the two candidates—$v_{\infty,\odot} = 21.5$ km s^{-1} and 16.9 km s^{-1}—sample the low end of the velocity distribution expected for objects from the Galactic solar neighborhood. For comparison, 1I/'Oumuamua entered the Solar System with $v_{\infty,\odot} \approx 26$ km s^{-1} (K. J. Meech et al. 2017) and 2I/Borisov with $v_{\infty,\odot} \approx 32$ km s^{-1} (P. Guzik et al. 2020), whereas 3I/ATLAS entered with $v_{\infty,\odot} \approx 58$ km s^{-1} 1 (D. Z. Seligman et al. 2025). The lower excess speeds of the fireball candidates are qualitatively consistent with the expectation that smaller, fainter impactors are preferentially detected at lower encounter speeds, as long as their atmospheric luminosity is sufficient to trigger space-based sensors.

4.3. Material Recovery Prospects

CNEOS-22 occurred over the open Pacific at $\sim$3–4 km depth, presenting deep-ocean recovery challenges similar to the IM1 expedition (A. Loeb et al. 2024). Its higher impact energy (0.69 kt) suggests a more massive impactor with potentially more recoverable debris than CNEOS-25. However, CNEOS-25's Arctic location (Barents Sea) offers the advantage of a shallow continental shelf ($\sim$200–400 m) but the constraints of sea-ice logistics. Crucially, CNEOS-25 is recent (February 2025), and rapid mobilization could maximize recovery prospects before material redistribution by ice drift and currents.

4.4. Implications for Interstellar Meteoroid Flux

Two detections over $\sim$7 years of post-2018 monitoring implies an Earth-impact rate on the order of $\sim$0.3 events yr^{-1} for meter-scale interstellar bolides at the CNEOS detection threshold, consistent with past expectations (A. Siraj & A. Loeb 2022b; E. Peña-Asensio & D. Z. Seligman 2025b; D. Jewitt & D. Z. Seligman 2023).

5. SUMMARY

We report two previously unrecognized interstellar meteor candidates in the post-2018 CNEOS fireball database, identified by computing heliocentric orbits from space-based velocity measurements and propagating measurement uncertainty through Monte-Carlo simulations calibrated to the empirical low-discrepancy error model of E. Peña-Asensio et al. (2025a):

Table 1. Properties of the two interstellar meteor candidates.

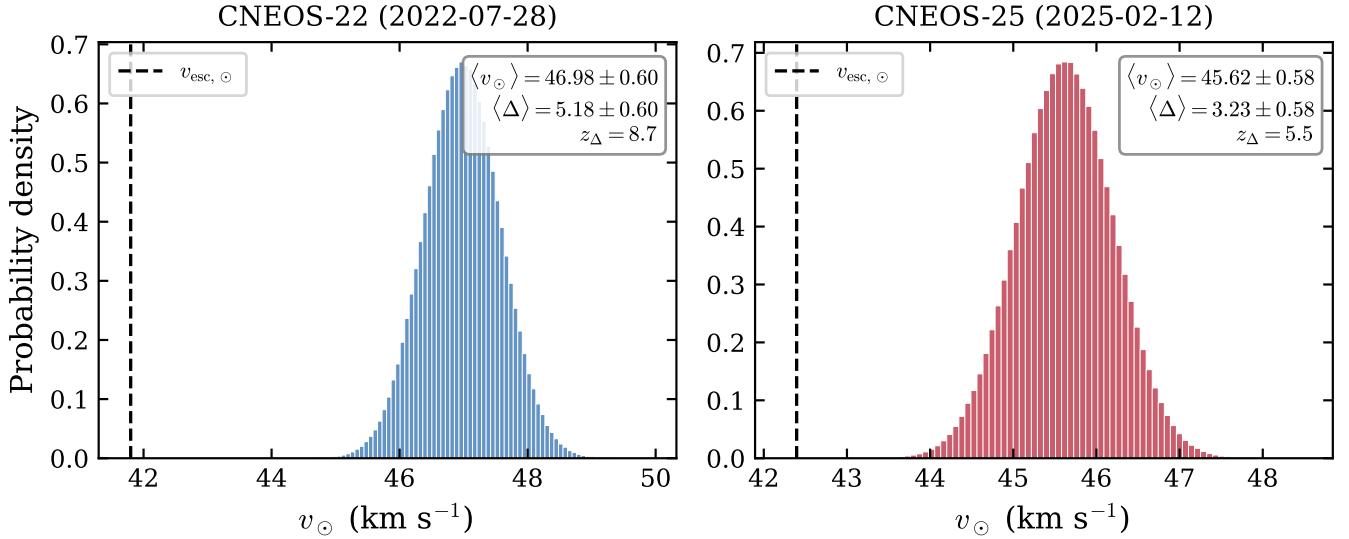| Property	CNEOS-22 (2022-07-28)	CNEOS-25 (2025-02-12)
Date/time (UTC)	2022-07-28 01:36:07	2025-02-12 04:33:39
Latitude	$-6.0°$ (S)	$+73.4°$ (N)
Longitude	$-86.9°$ (W)	$+49.3°$ (E)
Altitude (km)	37.5	42.0
Impact energy (kt)	0.69	0.13
Location	Pacific Ocean	Arctic (Barents Sea)
$v_\odot$ $(\mathrm{km\,s^{-1}})$	46.98	45.63
$v_{\mathrm{esc},\odot}$ $(\mathrm{km\,s^{-1}})$	41.79	42.40
$v_{\infty,\odot}$ $(\mathrm{km\,s^{-1}})$	21.5	16.9
$\varepsilon_\odot$ $(\mathrm{km^2\,s^{-2}})$	$+230$	$+142$
k_{bound} / N	0 / 10^6	0 / 10^6
p_{bound} (95% UL)	$< 3 \times 10^{-6}$	$< 3 \times 10^{-6}$
$\langle\Delta\rangle \pm \sigma_\Delta$ $(\mathrm{km\,s^{-1}})$	5.18 ± 0.60	3.22 ± 0.58
z_Δ	8.7	5.5

Figure 2. Monte-Carlo distributions of heliocentric speed $v_\odot$ for CNEOS-22 (2022-07-28; *left*) and CNEOS-25 (2025-02-12; *right*), based on 10^6 realizations of the E. Peña-Asensio et al. (2025a) low-discrepancy uncertainty model. The dashed vertical line marks the solar escape speed $v_{\mathrm{esc},\odot}$ at each event's heliocentric distance. In both cases the entire distribution lies above Solar System escape, with no bound realizations observed. Inserts provide the mean heliocentric speed (in km s^{-1}), the mean margin above escape $\langle\Delta\rangle$ (in km s^{-1}), and its statistical significance in units of standard deviations, z_Δ.

1. **CNEOS-22** (2022-07-28; eastern tropical Pacific): $v_\odot = 46.98$ km s^{-1}, $v_{\infty,\odot} = 21.5$ km s^{-1}, $z_\Delta = 8.7\sigma$ above escape.

2. **CNEOS-25** (2025-02-12; Barents Sea, Arctic): $v_\odot = 45.63$ km s^{-1}, $v_{\infty,\odot} = 16.9$ km s^{-1}, $z_\Delta = 5.5\sigma$ above escape.

For both events, none of 10^6 Monte-Carlo realizations yield a bound heliocentric orbit ($p_{\mathrm{bound}} < 3 \times 10^{-6}$ at 95% confidence), and the adopted error model would need to underestimate the true uncertainties by factors of 5–9 to render either candidate marginal. These are the strongest interstellar meteor candidates yet identified in the calibrated era of the CNEOS record. Follow-up N-body orbital reconstruction, fall-location model-
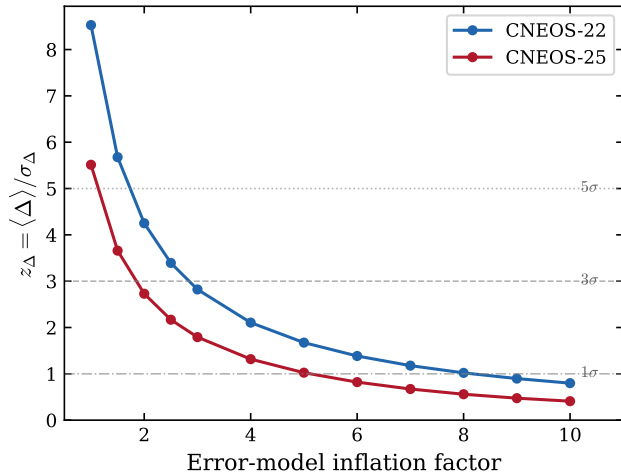
Figure 3. Sensitivity of the interstellar classification to systematic underestimation of CNEOS velocity uncertainties. The margin significance z_Δ is plotted as a function of a multiplicative inflation factor applied uniformly to all three uncertainty components (σ_v, σ_{RA}, σ_{Dec}). CNEOS-22 (2022-07-28) remains above 3σ until the errors are inflated by ∼3×, and above 1σ until ∼9×. CNEOS-25 (2025-02-12) crosses 3σ near ∼2× and 1σ near ∼5.5×.

ing, and—where feasible—material recovery expeditions are warranted, particularly for the recent CNEOS-25 event.

REFERENCES

Collaboration, A., Price-Whelan, A. M., Lim, P. L., et al. 2022, The Astrophysical Journal, 935, 167

Devillepoix, H. A., Bland, P. A., Sansom, E. K., et al. 2019, Monthly Notices of the Royal Astronomical Society, 483, 5166

Ginsburg, A., Sipőcz, B. M., Brasseur, C., et al. 2019, The Astronomical Journal, 157, 98

Giorgini, J., Yeomans, D., Chamberlin, A., et al. 1996, in AAS/Division for Planetary Sciences Meeting Abstracts# 28, Vol. 28, 25–04

Guzik, P., Drahus, M., Rusek, K., et al. 2020, Nature Astronomy, 4, 53

Harris, C. R., Millman, K. J., Van Der Walt, S. J., et al. 2020, nature, 585, 357

Jewitt, D., & Seligman, D. Z. 2023, Annual Review of Astronomy and Astrophysics, 61, 197, doi: 10.1146/annurev-astro-071221-054221

Loeb, A., Jacobsen, S. B., Tagle, R., et al. 2024, Chemical Geology, 670, 122415, doi: 10.1016/j.chemgeo.2024.122415

Meech, K. J., Weryk, R., Micheli, M., et al. 2017, Nature, 552, 378

Peña-Asensio, E., & Seligman, D. Z. 2025b, A&A, 704, L1, doi: 10.1051/0004-6361/202557337

Peña-Asensio, E., Trigo-Rodríguez, J. M., & Rimola, A. 2022, AJ, 164, 76, doi: 10.3847/1538-3881/ac75d2

Peña-Asensio, E., Socas-Navarro, H., & Seligman, D. Z. 2025a, Astronomy & Astrophysics, 701, A202

Seligman, D. Z., Micheli, M., Farnocchia, D., et al. 2025, The Astrophysical Journal Letters, 989, L36

Siraj, A., & Loeb, A. 2022a, ApJ, 939, 53, doi: 10.3847/1538-4357/ac8eac

Siraj, A., & Loeb, A. 2022b, The Astrophysical Journal Letters, 941, L28

Virtanen, P., Gommers, R., Oliphant, T. E., et al. 2020, Nature methods, 17, 261